Persoon Ann, M. (Orcid ID: 0000-0001-8161-2225)
Kurth William, S (Orcid ID: 0000-0002-5471-6202)
Gurnett Donald, A. (Orcid ID: 0000-0003-2403-0282)
Groene Joseph, B. (Orcid ID: 0000-0002-1252-4755)
Sulaiman Ali, H. (Orcid ID: 0000-0002-0971-5016)
Wahlund Jan-Erik (Orcid ID: 0000-0002-2107-5859)
Morooka Michiko, W. (Orcid ID: 0000-0001-9958-0241)
HADID Lina (Orcid ID: 0000-0002-8587-0202)
Waite Jack, Hunter (Orcid ID: 0000-0002-1978-1025)
Cravens Thomas, E. (Orcid ID: 0000-0003-0912-8353)

Electron Density Distributions in Saturn's Ionosphere

A. M. Persoon[1], W. S. Kurth[1], D. A. Gurnett[1], J. B. Groene[1], A. H. Sulaiman[1], J.-E. Wahlund[2], M. W. Morooka[2], L. Z. Hadid[2], A. F. Nagy[3], J. H. Waite, Jr.[4], and T. E. Cravens[5]

[1] Department of Physics and Astronomy, University of Iowa, Iowa City, IA, USA.

[2] Swedish Institute of Physics, Uppsala, Sweden

[3] Department of Atmospheric, Oceanic and Space Sciences, University of Michigan, Ann Arbor, MI, USA

[4] Southwest Research Institute, Space Science and Engineering Division, 6220 Culebra Road, San Antonio, TX, USA

[5] Department of Physics and Astronomy, University of Kansas, Lawrence, KS, USA

Corresponding author: Ann M. Persoon (ann-persoon@uiowa.edu)

Key Points:

- The first in-situ measurements of the electron density in the low to middle latitudes of Saturn's ionosphere
- Evidence of high orbit-to-orbit variability in the electron density profiles for all latitudes and for the higher altitudes of Cassini's Grand Finale orbits
- Evidence of a two-layered ionospheric electron density distribution up to an altitude of 15000 km
- Presentation of a scale height electron density model for a double-layered ionosphere for both the northern and southern hemispheres

This is the author manuscript accepted for publication and has undergone full peer review but has not been through the copyediting, typesetting, pagination and proofreading process, which may lead to differences between this version and the Version of Record. Please cite this article as doi: 10.1029/2018GL078020

Abstract

Between 26 April and 15 September 2017 Cassini executed 23 highly-inclined Grand Finale orbits through a new frontier for space exploration, the narrow region between Saturn and the D Ring, providing the first opportunity for obtaining *in situ* ionospheric measurements. During the Grand Finale orbits, the Radio and Plasma Wave Science (RPWS) instrument observed broadband whistler mode emissions and narrowband upper hybrid frequency emissions. Using known wave propagation characteristics of these two plasma wave modes, the electron density is derived over a broad range of ionospheric latitudes and altitudes. A two-part exponential scale height model is fitted to the electron density measurements. The model yields a double-layered ionosphere with plasma scale heights of 545/575 km for the northern/southern hemispheres below 4500 km and plasma scale heights of 4780/2360 km for the northern/southern hemispheres above 4500 km. The interpretation of these layers involves the interaction between the rings and the ionosphere.

Introduction

Our knowledge of the vertical distribution of Saturn's ionospheric electron densities before Cassini's Grand Finale came from remote observations using radio occultation measurements. The radio occultation technique yields the vertical structure of the electron density distribution from which a plasma scale height is derived. Between 1979 and 1981, Pioneer (Kliore et al., 1980) and the two Voyager spacecraft (Atreya et al., 1984; Lindal et al., 1985) employed radio occultation measurements during flybys of Saturn to probe the ionosphere on six occasions. When Cassini arrived at Saturn in 2004, remote probing of the planet's ionosphere using the radio occultation technique resumed and 59 new vertical electron density profiles were derived (Nagy et al., 2006; Kliore et al., 2009; 2014). A correlation between the RPWS equatorial electron densities and electron densities from Cassini equatorial radio occultations can be seen in Figure S1.

Radio occultation measurements over a wide range of latitudes, altitudes and local times determined that there was a significant variability in the electron density profiles (Kliore et al., 2009; Nagy et al., 2009); that the electron density increased with increasing latitude (Kliore et al., 2009); and that there was a strong diurnal variation in the electron density profiles (Kliore et al., 2009; Nagy et al., 2006). The presence of the diurnal density variation was also inferred from the low-frequency cutoff of the Saturn Electrostatic Discharges (SEDs) measured by Voyager (Kaiser et al., 1984) and Cassini (Fischer et al., 2008; 2011), although the implied variations are quite significantly different.

Cassini's 23 Grand Finale orbits in 2017 spanned five months and carried Cassini deep into Saturn's ionosphere, enabling the Cassini instruments to obtain the first *in situ* measurements of Saturn's ionospheric plasma. RPWS Langmuir Probe (RPWS/LP) electron density measurements revealed a highly variable ionosphere with significant fine structure in the electron density profiles and a strong north/south asymmetry due to ring shadow effects (Hadid et al., 2018b; Wahlund et al., 2018a). Using RPWS electron plasma frequency measurements derived from the upper frequency cutoff of the whistler mode emissions, Sulaiman et al. (2017) derived the lower hybrid frequency. They were able to identify the intense electrostatic waves and their harmonics in Saturn's topside ionosphere as rarely-observed lower hybrid waves, which scale with the lower hybrid frequency. In this paper we present RPWS electron density measurements over a range of ionospheric latitudes and altitudes which have been derived from the propagation characteristics of whistler mode and upper hybrid resonance emissions. Two scale height electron density models for the northern and southern hemispheres will demonstrate that there is a higher-altitude transport layer above ~4500 km and a lower-altitude ionospheric layer below ~4500 km that is composed of a chemistry-dominated region below 2500 km and a complex region between 2500 km and 4500 km with a "layered" ion distribution that may include both chemistry and transport processes.

RPWS Electron Density Analysis

Figure 1 is a close-up meridional view of the tightly-grouped Grand Finale orbits and the Final Plunge into Saturn's atmosphere (orbit 293). The orbits are color-coded, based on the distance from Saturn at Cassini's minimum altitude or closest approach. The orbits are grouped into low-altitude, mid-altitude and high-altitude orbits. Throughout this manuscript, altitude is measured along the vertical above the one-bar pressure level in Saturn's atmosphere. The one-bar pressure level represents Saturn's ellipsoidal surface where the equatorial radius is 60,268 km and the polar radius is 54,364 km [see Table IV in Archinal et al. (2011)]. The low-altitude orbits consist of the final five orbits which brought Cassini deep into Saturn's upper atmosphere (orbits 288-292) as well as the Final Plunge (orbit 293). These orbits span an altitude range of 1494 km to 1712 km at Cassini's closest approach. The mid-altitude orbits (orbits 271-275 and orbits 283-287) span an altitude range of 2697 km to 2948 km. The high-altitude orbits, where Cassini crossed the ring plane through the inner fringe of the D Ring (orbits 276-282), span an altitude range of 3349 km to 3893 km. For the Grand Finale orbits, closest approach occurs in the southern hemisphere over a latitude range of -3.9° to -5.3° within a narrow two-hour range of local times centered on local noon. For all of these orbits, altitude and latitude are highly correlated with higher latitudes measured at higher altitudes.

Cassini's Radio and Plasma Wave Science instrument (RPWS) made *in situ* observations of broadband electromagnetic whistler mode emissions that provide electron density measurements in Saturn's ionosphere over a range of ionospheric latitudes and altitudes. These whistler mode emissions are known to propagate over a broad range of frequencies and are driven into resonance (the upper frequency cutoff) at the electron plasma frequency (f_{pe}) in low-density regions where the electron plasma frequency is less than the electron cyclotron frequency (f_{ce}) (Gurnett et al., 1983). The electron density (n_e in cm^{-3}) is derived from the electron plasma frequency (in Hz) using $f_{pe} = 8980\sqrt{n_e}$. When Cassini began the final five orbits in August 2017 and entered the high-density region of Saturn's lower ionosphere, the whistler mode emissions were heavily damped and not driven into resonance at the electron plasma frequency. But, in this high-density region where $f_{pe} > f_{ce}$, RPWS observed an emission band above the electron cyclotron frequency which propagates at the upper hybrid resonance frequency (f_{UH}). The electron plasma frequency, and subsequently the electron density, is derived from the upper hybrid resonance frequency using $f_{UH}^2 = f_{pe}^2 + f_{ce}^2$ where all frequencies are given in Hz (Persoon et al., 2005).

Figure 2a illustrates both plasma wave modes for the first of the final five orbits on 14 August 2017. The broadband whistler mode emissions, which are present throughout the Grand Finale orbits, show a sharp upper frequency cutoff at the electron plasma frequency (f_{pe}) at higher latitudes where the upper frequency cutoff is well below f_{ce}. However, between 04:14 and 04:30 the upper frequency cutoff is neither sharp nor well-defined. Cassini has entered the high-density region of Saturn's upper atmosphere and the heavily damped whistler mode emissions are not driven into resonance at the electron plasma frequency. During this same time interval, RPWS observes the narrowband upper hybrid resonance (f_{UH}) emissions above the electron cyclotron frequency (f_{ce}). The electron density is derived from wave propagation characteristics of these two plasma wave modes and is shown in panel b. The error bars indicate the uncertainty in determining the electron plasma frequency and the upper hybrid resonance frequency. The uncertainty varies from 9% to 19% of the electron density measurements.

RPWS Electron Density Distributions in Saturn's Ionosphere

The RPWS electron density measurements for all of the Grand Finale orbits are shown on a common latitude plot in Figure 3a. As in Figure 1, the latitudinal electron density profiles are color-coded according to the altitude of Cassini at closest approach. The final five latitudinal electron density profiles show consistently reproducible electron density measurements at low

latitudes, with peak densities just below 10^4 cm^{-3}, consistent with peak densities obtained in the Pioneer, Voyager and Cassini radio occultation measurements (Kliore et al., 1980, 2009; Lindal et al., 1985; Nagy et al., 2006). At higher latitudes, the latitudinal electron density profiles show strong variability from orbit-to-orbit, spanning up to two orders of magnitude. This variability has been previously noted in the radio occultation observations (Kliore et al., 2009; Nagy et al., 2009). The orbit-to-orbit variability may be due to longitudinal differences in the orbits, especially at higher latitudes. But a strong contributing factor leading to temporal electron density variations is likely to be the dynamic nature of Saturn's ionosphere and the ring-ionosphere interaction (Hadid et al., 2018a). Variability in the photolytic processes acting on the ring atmosphere and ionosphere and/or meteoroid impacts on the ring surface could cause temporal changes in the electron density through these interactions.

The latitudinal electron density profiles also show a significant north-south asymmetry in the latitude distribution due, in part, to the ring shadow effect in the southern hemisphere. The shadows of the opaque A and B rings result in reduced ionization in the upper atmosphere and associated electron density depletions (Wahlund et al., 2018a; Hadid et al., 2018b). Hadid et al. (2018a) also notes a strong electrodynamic ring-ionosphere interaction associated with the highly variable electron density profiles above 1.11 R_S in the southern hemisphere.

There are two places in Figure 3a where the altitude dependence of the electron density distributions can be separated from the latitude dependence. From 10º S to 5º N, there is a strong half-order of magnitude difference between the closely-grouped peak electron density measurements in the low-altitude final five orbits and the highest electron densities seen in the remaining Grand Finale orbits. There is a similar difference between the very low-altitude electron density measurements obtained during the Final Plunge at 10º N and the highest electron densities at the same latitude for the other orbits. Figure 3b shows the same electron density measurements averaged in bins of 2º latitude for the same four color-coded groups of orbits. The altitude dependence of the electron density distributions is apparent at low latitudes. The averaged latitudinal electron density profiles show the strongest and most consistent altitude dependence within 10º of the ring plane, with the highest electron densities measured in the final five orbits (in red) and the lowest electron densities measured in the D Ring orbits (in black).

Scale Height Density Models for Saturn's Northern and Southern Ionosphere

An inspection of the electron density measurements as a function of altitude yields information about Saturn's ionospheric layers and the altitude of the transition between the layers. Figure 4a shows all of the Grand Finale electron density measurements as a function of altitude. The data

measurements are divided between the northern hemisphere (in red) and the southern hemisphere (in blue). All electron density measurements for the Final Plunge (solid black line) are in the northern hemisphere. The data distribution clearly shows the electron densities increasing with decreasing altitude. There is very little spread in the data at the lowest altitudes but the variability increases to more than an order of magnitude at higher altitudes. The north-south asymmetry, attributed to the reduced ionization and electron density depletions in the southern hemisphere from the ring shadow effect, are evident in the divergence in the north and south distributions above 3000 km.

An ionospheric plasma scale height model is derived from the altitude distribution of the RPWS electron density measurements. Figure 4b shows the same northern and southern densities averaged in altitude bins of 500 km and a classic ionospheric electron density distribution with two ionospheric layers. The plasma scale height model is fitted to these averaged data values using a two-part exponential equation: $n_e = n_1 e^{-h/H_1} + n_2 e^{-h/H_2}$ where n_1 and n_2 are the y intercepts, h is the altitude, and H_1 and H_2 are the plasma scale heights. The subscript 1 refers to the ionospheric layer at the lower altitudes and the subscript 2 refers to the ionospheric layer at the higher altitudes. The fit to the averaged electron density values clearly shows a transition from the lower-altitude layer to the higher-altitude ionospheric layer at ~4500 km. The error bars represent one standard deviation in the fit of the plasma scale height model to the binned and averaged data. The fit of the two-part exponential scale height equation to these averaged electron densities yields plasma scale heights of 545 km and 575 km for the lower ionospheric layer in the northern and southern hemispheres respectively and plasma scale heights of 4780 km and 2360 km for the higher ionospheric layer in the northern and southern hemispheres respectively. Figure S2 shows the distribution of the RPWS electron density measurements at 4500 km. The transition to the transport-dominated region at ~4500 km occurs along field lines that map back to region just inside the inner edge of the D Ring.

We should note here that diffusive equilibrium conditions are expected to be present along strong magnetic field lines (Schunk & Nagy, 2009). In its highly-inclined orbit, Cassini crosses numerous field lines rapidly. Because altitude is measured vertically from the "surface" of the one-bar pressure level, the altitudinal electron density distribution is not aligned along Saturn's magnetic field lines. The plasma scale heights determined from the altitude distribution of the electron densities in Figure 4 are a useful description of the electron density distribution but cannot be interpreted as vertical scale heights in the conventional sense.

Understanding Saturn's Ionospheric Layers

The classic picture of a planetary ionosphere is one with a lower ionospheric layer dominated by ionospheric chemistry interactions between the neutrals and the ions and an upper transport-dominated layer of highly diffusive light ions (Schunk & Nagy, 2009). Current Cassini *in situ* measurements of heavy molecular neutrals and ions have revealed a more complex picture of Saturn's ionosphere. The dramatic shift in the slope of the electron distribution and in the resulting plasma scale height at ~4500 km (Figure 4b) clearly shows a transition to a high-altitude transport region where the highly diffusive light ions dominate. But this transition is occurring several thousand kilometers above the expected transition at ~ 2500 km that would separate the heavy molecular ion layer in photochemical equilibrium (the PCE layer) from the light ion transport layer. Below ~2500 km, the upper atmosphere is dominated by heavy molecular ions and neutrals from Saturn's atmosphere in near photochemical equilibrium (Moore et al., 2018; Morooka et al., 2018; Wahlund et al., 2018b; Waite et al., 2018). Photochemical analyses (Cravens et al., 2018; Moore et al., 2018) ~~derives~~ derive the distributions of these heavy molecular ions in Saturn's equatorial ionosphere, which have been inferred from the differences between the light ion densities and the electron densities (Morooka et al., 2018; Wahlund et al., 2018b; Waite et al., 2018).

Above 2500 km, *in situ* measurements of heavy molecular neutrals and ions have revealed a more complex picture of Saturn's lower ionospheric layer. The factor contributing to the complexity of the lower ionospheric layer between 2500 km and 4500 km is the dynamic interaction of the rings with Saturn's ionosphere. This interaction was theorized in early models to explain the lower peak electron densities observed in the Pioneer and Voyager radio occultations (Kliore et al., 1980; Lindal et al., 1985). The most popular explanation to reduce the light ion densities in early models to correlate with the radio occultation density measurements was the introduction of charged water particles from the rings into Saturn's midlatitude ionosphere, called "ring rain" (Connerney & Waite, 1984; O'Donoghue et al., 2017). O'Donoghue et al. (2017) detected latitudinal variations in the signature of midlatitude ionospheric H_3^+ ions consistent with an influx of electrically charged water particles from the rings along magnetic field lines mapping to the inner edges of the B and A rings and the Enceladus orbit. *In situ* measurements by Cassini's Ion and Neutral Mass Spectrometer (INMS), the Magnetosphere Imaging Instrument (MIMI) and the RPWS/ Langmuir Probe instrument observed an influx of heavy neutrals and dust grains from the rings into Saturn's ionosphere at equatorial latitudes (Mitchell et al., 2018; Wahlund et al., 2018b; Waite et al., 2018). Waite et al. (2018) discovered an influx of heavy molecular neutrals into Saturn's equatorial ionosphere at an altitude of ~3600 km, an ionospheric region already dominated by H^+ and H_3^+ ions. The dominance of these highly diffusive light ions suggests that the ionospheric region above 2500

km is a transport region. However, the ionospheric scale height model does not show the significant change in the slope of the electron density distribution at 2500 km that would be expected for a transition between the chemistry-dominated PCE layer and a transport-dominated layer.

INMS measurements of heavy neutrals have shown that these ring particles are present in Saturn's equatorial ionosphere up to altitudes of ~3600 km (Waite et al., 2018). However, it should be noted that INMS measurements of these neutrals are not available above 3600 km. It is probable that the ring particles are present in the equatorial ionosphere out to the D Ring and possible that they are chemically interacting with the light ions that populate the region as they fall inward toward Saturn. Above the equatorial ionosphere, the ionospheric plasma is composed only of highly-diffusive light ions. There are "layers" in the lower ionosphere between 2500 and 4500 km, with different ion and neutral compositions and likely different chemistry/transport processes.

Summary

The fit of the two-part exponential scale height density model to the RPWS ionospheric electron densities shows a double-layered Saturn ionosphere for both the northern and southern hemispheres. The low-altitude layer below 4500 km is similar in both the northern and southern hemispheres with derived scale heights of 545 km and 575 km respectively, in agreement with the scale height at similar altitudes for the Final Plunge (Hadid et al., 2018a). It is also similar to the value of 500 km from earlier dusk radio occultation observations (Nagy et al., 2006). The north-south asymmetry in the electron distributions with increasing altitude above 4500 km results in very dissimilar scale heights of 4780 km and 2360 km respectively. The plasma scale height of 4780 km for the northern hemisphere compares well with the scale height of 4500 km for the higher-altitude ionospheric region in the northern hemisphere determined by Hadid et al. (2018a).

The interpretation of the plasma scale height must be considered with some caution when using the Grand Finale trajectories, as mentioned earlier. In these highly-inclined Grand Finale orbits, Cassini is rapidly crossing many field lines in passing through the ionosphere. The altitude distribution of the ionospheric electrons shown in Figure 4 does not reflect plasma diffusing along magnetic field lines and may be better interpreted as a distribution of electrons that is defined by the chemistry and transport processes in Saturn's ionosphere.

Chemistry dominates below 2500 km where the heavy molecular ions are in photochemical equilibrium. Transport dominates above 4500 km in a region populated by very diffusive light ions. Between 2500 and 4500 km is a "layered" ionospheric region with an influx of heavy neutrals and ions from the rings near the equatorial plane and a layer of diffusive H^+ and H_3^+ ions dominating the ionosphere above the equatorial layer. It is likely that, in the equatorial layer, the ring particles are chemically interacting with H^+ and H_3^+ as they fall inward toward Saturn. The layer above the equatorial layer is likely a transport-dominated region populated by the highly diffusive light ions.

The ionospheric scale height model shows the expected classic transition to a transport-dominated ionospheric layer at ~4500 km, near the inner edge of the D Ring. However, the model shows a consistent slope in the electron distribution from the last Final Plunge density measurement at 1520 km up to 4500 km, with no discernible transition at the upper boundary of the PCE layer at 2500 km. How to interpret the low-altitude ionosphere between 2500 km and 4500 km is still under investigation.

Acknowledgements

The research at the University of Iowa was supported by NASA through Contract 1415150 with the Jet Propulsion Laboratory (JPL). Research at the Swedish Institute of Physics is supported by the Swedish National Space Board. Research at the University of Michigan was supported by NASA through JPL Contract 1416972. The research at the University of Kansas was supported by NASA Prime Contract NAS7-03001 under JPL Subcontract 1405853 to the Southwest Research Institute and SWRI subcontract to the University of Kansas. The Cassini RPWS electron density data are scheduled to be archived at the NASA Planetary Data System website http://pds.nasa.gov or are available upon request from the author.

References

Archinal, B. A., A'Hearn, M. F., Bowell, E., Conrad, A., Consolmagno, G. J., Courtin, R., Fukushima, T., Hestroffer, D., Hilton, J. L., Krasinsky, G. A., Neumann, G., Oberst, J., Seidelmann, D. K., Stooke, P., Tholen, D. J., Thomas, P. C., & Williams, I. P. (2011). Report of the IAU Working Group on Cartographic Coordinates and Rotational Elements: 2009. *Celestial Mechanics and Dynamical Astronomy*, *109*, 101-135, doi:10.1007/s10569-010-9320-4.

Atreya, S. K., Waite, J. H., Donahue, T. M., Nagy, A. F., & McConnell, J. C. (1984). Theory, measurements, and models of the upper atmosphere and ionosphere of Saturn. In T. Gehrels & M. S. Matthews (Eds.), *Saturn* (pp. 239-277), Tucson: University of Arizona Press.

Connerney, J. E. P., & Waite, J. H. (1984). New model of Saturn's ionosphere with an influx of water from the rings. *Nature, 312,* 136-138, doi:10.1038/312136a0.

Cravens, T. E., Moore, L., Waite, J. H., Perryman, R., Perry, M., Wahlund, J.-E., Persoon, A., & Kurth, W. (2018). The ion composition of Saturn's equatorial ionosphere as observed by Cassini. *Geophysical Research Letters*, this issue, https://doi.org/10.1029/2018GL077868.

Fischer, G., Gurnett, D. A., Kurth, W. S., Akalin, F., Zarka, P., Dyudina, U. A., Farrell, W. M., & Kaiser, M. L. (2008). Atmospheric electricity at Saturn. *Space Science Reviews, 137,* https://doi.org/10.1007/s11214-008-9370-z.

Fischer, G., Gurnett, D. A., Zarka, P., Moore, L., & Dyudina, U. A. (2011). Peak electron densities in Saturn's ionosphere derived from the low-frequency cutoff of Saturn lightning. *Journal of Geophysical Research, 116,* https://doi.org/10.1029/2010JA016187.

Gurnett, D. A., Shawhan, S. D., & Shaw, R. R. (1983). Auroral hiss, Z mode radiation, and auroral kilometric radiation in the polar magnetosphere: DE 1 observations. *Journal of Geophysical Research, 88,* 329-340, https://doi.org/10.1029/JA088iA01p00329.

Hadid, L. Z., Morooka, M. W., Wahlund, J.-E., Persoon, A. M., Andrews, D. J., Shebanits, O., Kurth, W. S., Vigren, E., Edberg, N. J. T., Nagy, A. F., & Eriksson, A. I. (2018a). Saturn's ionosphere: Electron density altitude profiles and D ring interaction from the Cassini Grand Finale. *Geophysical Research Letters*, this issue, https://doi.org/10.1029/2018GL078004.

Hadid, L. Z., Morooka, M. W., Wahlund, J.-E., Moore, L., Cravens, T. E., Hedman, M. M., Edberg, N. J. T., Vigren, E., & Kurth, W. S. (2018b). A and B ring shadowing effects on Saturn's ionosphere: Implications for ring opacity and plasma transport processes. *Geophysical Research Letters, this issue*.

Kaiser, M. L., Desch, M. D., & Connerney, J. E. P. (1984). Saturn's ionosphere: Inferred electron densities. *Journal of Geophysical Research, 89* (A4), 2371-2376, https://doi.org/10.1028/JA089iA04p02371.

Kliore, A. J., Patel, I. R., Lindal, G. F., Sweetnam, D. N., Hotz, H. B., Waite, J. H., & McDonough, T. R. (1980). Structure of the ionosphere and atmosphere of Saturn from Pioneer

11 Saturn radio occultation. *Journal of Geophysical Research, 85,* 5857-5870, https:doi.org/10.1029/JA085iA11p05857.

Kliore, A. J., Nagy, A. F., Marouf, E. A., Anabtawi, A., Barbinis, E., Fleischman, D. U., & Kahan, D. S. (2009). Midlatitude and high-latitude electron density profiles in the ionosphere of Saturn by Cassini radio occultation observations. *Journal of Geophysical Research, 114*, https://doi.org/10.1029/2008JA013900.

Kliore, A. J., Nagy, A., Asmar, S., Anabtawi, A., Barbinis, E., Fleischman, D., Kahan, D., & Klose, J. (2014). The ionosphere of Saturn as observed by the Cassini Radio Science System. *Geophysical Research Letters, 41,* 5778-5782, https://doi.org/10.1002/2014GL060512.

Lindal, G. F., Sweetnam, D. N., & Eshleman, V. R. (1985). The atmosphere of Saturn: An analysis of the Voyager radio occultation measurements. *The Astronomical Journal, 90,* doi:10.1086/113820.

Mitchell, D. G., Perry, M. E., Hamilton, D. C., Westlake, J. H., Kollmann, P., Smith, H. T., Carbary, J. F., Waite, J. H., Perryman, R., Hsu, H.-W., Wahlund, J.-E., Morooka, M. W., Hadid, L. Z., Persoon, A. M., & Kurth, W. S. (2018). D-ring dust falling into Saturn's equatorial upper atmosphere. Submitted to *Science*.

Moore, L., Cravens, T. E., Mueller-Wodarg, I., Perry, M., Waite, H., Perryman, R., Nagy, A., Mitchell, D., Persoon, A., Wahlund, J.-E., & Morooka, M. W. (2018). Saturn's equatorial ionosphere: dominance of heavy ions and model comparisons with Cassini Grand Finale data. *Geophysical Research Letters, this issue.*

Morooka, M. W., Wahlund, J.-E., Hadid, L., Edberg, N., Vigren, E., Andrews, D., Persoon, A. M., Kurth, W. S., Gurnett, D. A., Farrell, W., Waite, J. H., Perryman, R. S., Perry, M., Mitchell, D. G., & Hsu, S. (2018). Saturn's dusty ionosphere of heavy ions. *Geophysical Research Letters, this issue*.

Nagy, A. F., Kliore, A. J., Marouf, E., French, R., Flasar, M., Rappaport, N. J., Anabtawi, A., Asmar, S. W., Johnston, D., Barbinis, E., Goltz, G., & Fleischman, D. (2006). First results from the ionospheric radio occultations of Saturn by the Cassini spacecraft. *Journal of Geophysical Research, 111*, https://doi.org/10.1029/2005JA011519.

Nagy, A. F., Kliore, A. J., Mendillo, M., Miller, S., Moore, L., Moses, J. I., Mueller-Wodarg, I., & Shemansky, D. (2009). Upper atmosphere and ionosphere of Saturn. In Dougherty, M. K.,

Esposito, L. W., & Krimigis, S. M. (Eds.), *Saturn from Cassini-Huygens* (pp. 181-201), Dordrecht: Springer, https://doi.org/10.1007/978-1-4020-9217-6_8.

O'Donoghue, J., Moore, L., Connerney, J. E. P., Melin, H., Stallard, T. S., Miller, S., & Baines, K. H. (2017). Redetection of the ionospheric H_3^+ signature of Saturn's "Ring Rain". *Geophysical Research Letters, 44*, https://doi.org/10.1002/2017GL075932.

Persoon, A. M., Gurnett, D. A., Kurth, W. S., Hospodarsky, G. B., Groene, J. B., Canu, P., & Dougherty, M. K. (2005). Equatorial electron density measurements in Saturn's inner magnetosphere. *Geophysical Research Letters, 32*, https://doi.org/10.1029/2005GL024294.

Schunk, R. W., & Nagy, A. F. (2009). *Ionospheres: Physics, Plasma Physics, and Chemistry*, 2nd Edition. United Kingdom: Cambridge University Press, https://doi.org/10.1017/CB09780511635342.

Sulaiman, A. H., Kurth, W. S., Persoon, A. M., Menietti, J. D., Hospodarsky, G. B., Farrell, W. M., Gurnett, D. A., & Hadid, L. Z. (2017). Intense harmonic emissions observed in Saturn's ionosphere. *Geophysical Research Letters, 44*, https://doi.org/10.1002/2017GL076184.

Wahlund, J.-E., Morooka, M. W., Hadid, L. Z., Persoon, A. M., Farrell, W. M., Gurnett, D. A., Hospodarsky, G. B., Kurth, W. S., Ye, S.-Y., Andrews, D. J., Edberg, N. J. T., Eriksson, A. I., & Vigren, E. (2018a). In situ measurements of Saturn's ionosphere show it is dynamic and interacts with the rings. *Science*, doi:10.1126/science.aao4134.

Wahlund, J.-E., Vigren, E., Morooka, M. W., Hadid, L. Z., Farrell, W. M., Persoon, A. M., Kurth, W. S., Gurnett, D. A., Mitchell, D. G., Waite, J. H., Moore, L., Cravens, T. E., Galand, M., & Nagy, A. F. (2018b). On the characteristics of charged dust in Saturn's equatorial ionosphere – Implications from Cassini RPWS/LP data. *Geophysical Research Letters, this issue.*

Waite, J. H., Perryman, R., Perry, M., Miller, K., Bell, J., Cravens, T. E., Glein, C. R., Grimes, J., Hedman, M., Brockwell, T., Teolis, B., Moore, L., Mitchell, D., Persoon, A., Kurth, W., Wahlund, J.-E., Morooka, M., Hadid, L., Chocron, S., Nagy, A., Yelle, R., Ledvina, S., & Johnson, R. (2018). Chemical interactions between Saturn's atmosphere and rings. Submitted to *Science*.

Figure Captions

Figure 1. A meridional plot in cylindrical coordinates showing the tightly-grouped Cassini trajectories for all of the Grand Finale orbits. The trajectories are shown in four time-sequenced groups and color-coded according to the altitude of Cassini at closest approach.

Figure 2. Panel a is a color RPWS spectrogram for orbit 288 illustrating both the broadband whistler mode emissions and the narrowband upper hybrid resonance (f_{UH}) emissions. Electron density measurements are obtained from the wave propagation characteristics of these plasma wave modes. Panel b shows the electron density measurements derived from these plasma wave spectral features.

Figure 3. Panel a shows the latitudinal distributions of the RPWS electron density measurements for all of the Grand Finale orbits. The latitudinal electron density profiles are color-coded according to the altitude of Cassini at closest approach. These latitudinal profiles show strong variability from orbit-to-orbit, up to two orders of magnitude, as well as a significant north-south asymmetry due, in part, to the ring shadow effect in the southern hemisphere. Panel b shows the electron density measurements for the four groupings of the Grand Finale orbits averaged in latitude bins of 2º. The averaged latitudinal electron density profiles show a strong altitude dependence within 10º of the ring plane.

Figure 4. The altitude distribution of the RPWS electron density profiles for all of the Grand Finale orbits. Panel a shows the density measurements for the northern hemisphere in red; the density measurements for the southern hemisphere in blue and the density measurements for Cassini's plunge into Saturn's upper atmosphere (part of the northern data set) as a solid black line. There is very little spread at the lowest altitudes for both hemispheres but the variability increases at higher altitudes. The north-south asymmetry, attributed to the reduced ionization and electron density depletions in the southern hemisphere from the ring shadow effect, is evident in the divergence in the north and south distributions above 3000 km. Panel b shows the same data averaged in altitude bins of 500 km and a classic ionospheric density distribution with two ionospheric layers. The fit of the scale height model to the averaged data uses a two-part exponential equation: $n_e = n_1 e^{-h/H_1} + n_2 e^{-h/H_2}$ where the subscript 1 refers to the ionospheric layer at the lower altitudes and the subscript 2 refers to the ionospheric layer at the higher altitudes.

A-D17-099-5

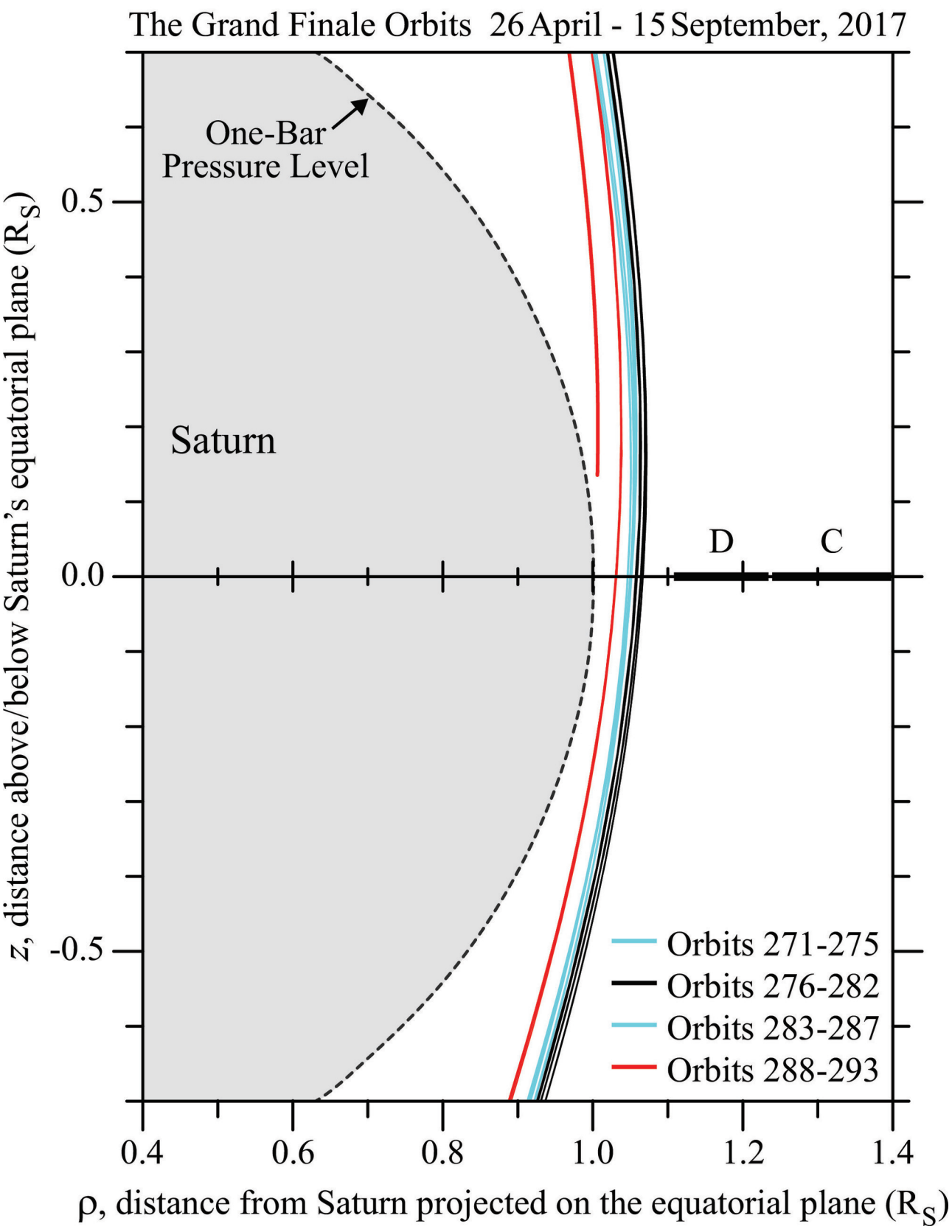

2018gl078020-f01-z-.eps

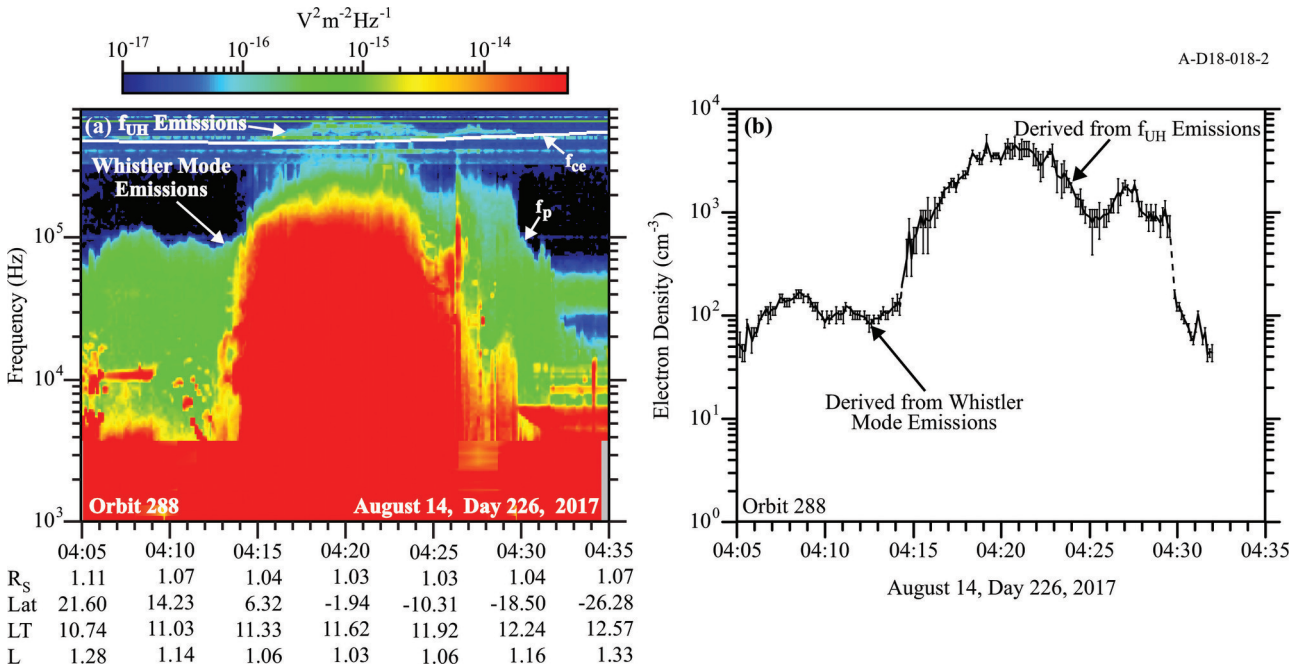

2018gl078020-f02-z-.eps

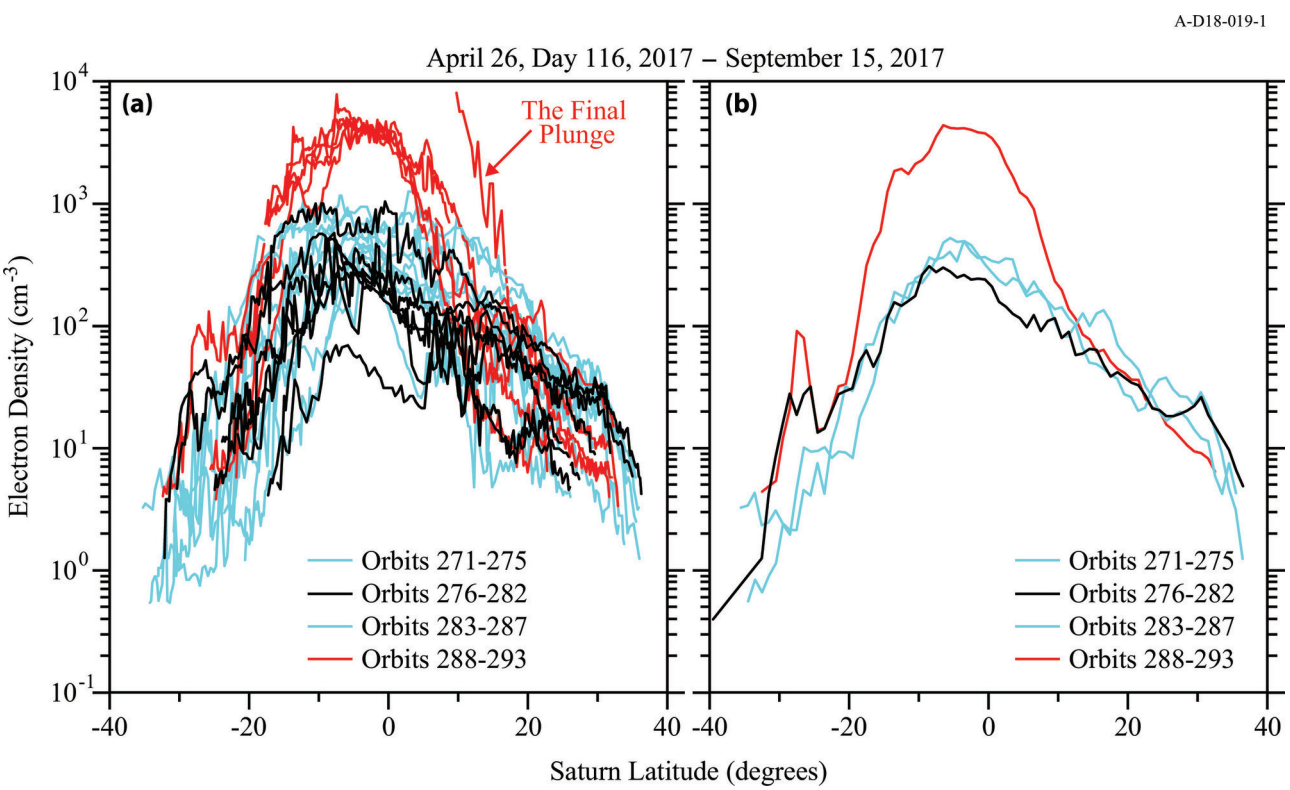

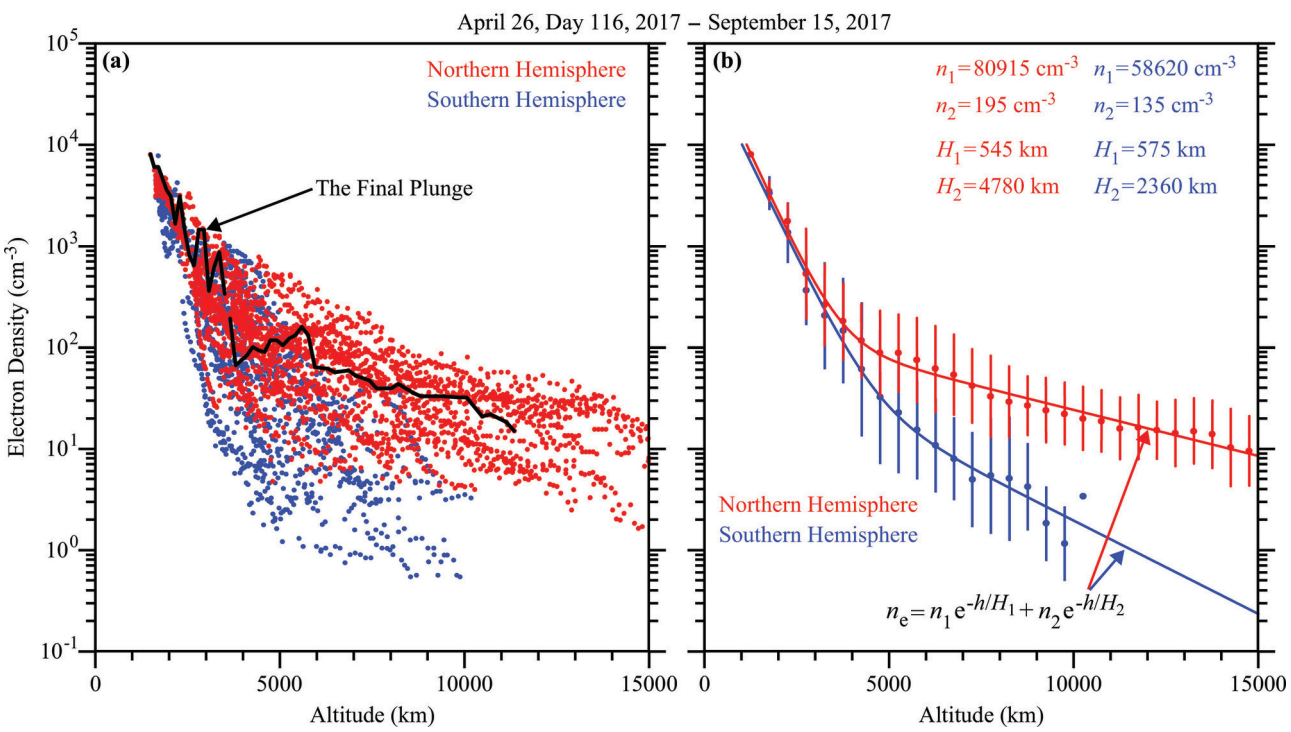

2018gl078020-f04-z-.eps